

# Magnetoelectric effects in ferrite-lead zirconate titanate layered composites: The influence of zinc substitution in ferrites

G. Srinivasan, E. T. Rasmussen, and R. Hayes

*Physics Department, Oakland University, Rochester, Michigan 48309-4401*

(Received 26 February 2002; revised manuscript received 6 November 2002; published 22 January 2003)

The observation of strong magnetoelectric (ME) coupling is reported in zinc-substituted layered composites of ferrites and lead zirconate titanate (PZT). Multilayer samples contained cobalt zinc ferrite  $\text{Co}_{1-x}\text{Zn}_x\text{Fe}_2\text{O}_4$  (CZFO) ( $x=0-0.6$ ) or nickel zinc ferrite  $\text{Ni}_{1-x}\text{Zn}_x\text{Fe}_2\text{O}_4$  (NZFO) ( $x=0-0.5$ ) and were prepared by laminating and sintering ferrite and PZT thick films obtained by tape casting. The ME voltage coefficient  $\alpha_E$  was measured for transverse and longitudinal field orientations for frequencies 10–1000 Hz. A substantial enhancement in  $\alpha_E$  is observed with the substitution of Zn. The largest increase, by about 500%, is observed in CZFO-PZT and the smallest increase of 60% is measured for NZFO-PZT. As the Zn concentration is increased,  $\alpha_E$  increases and shows a maximum for  $x=0.2-0.4$ , depending on the ferrite. The data is analyzed based on a theoretical model for a ferrite-PZT bilayer, taking into consideration less than ideal coupling at the interface. The interface coupling parameter  $k$  is quite small for CZFO-PZT; it increases from 0 to 0.6 as Zn concentration is increased from 0% to 40%. Composites of NZFO-PZT, however, have a near perfect interface coupling. The Zn-assisted enhancement in the ME coefficient is discussed in terms of joule magnetostriction, initial permeability, and magnetomechanical coupling for the ferrites.

DOI: 10.1103/PhysRevB.67.014418

PACS number(s): 75.80.+q, 75.70.-i, 77.55.+f

## I. INTRODUCTION

The magnetoelectric (ME) effect is defined as the dielectric polarization of a material in an applied magnetic field or an induced magnetization in an external electric field. The induced polarization  $\mathbf{P}$  is related to the magnetic field  $\mathbf{H}$  by the expression  $\mathbf{P}=\alpha\mathbf{H}$ , where  $\alpha$  is the second-order ME-susceptibility tensor. The effect, first observed in antiferromagnetic  $\text{Cr}_2\text{O}_3$ , is weak in single-phase compounds.<sup>1</sup> Composites are desirable for the synthesis of materials with unique or improved properties.<sup>2</sup> A composite of piezomagnetic-piezoelectric phases is expected to be magnetoelectric since  $\alpha=\delta P/\delta H$  is the product of the piezomagnetic deformation  $\delta z/\delta H$  and the piezoelectric charge generation  $\delta Q/\delta z$ . We are interested in the dynamic ME effect; for an ac magnetic field  $\delta H$  applied to a biased sample, one measures the field  $\delta E$ . The ME voltage coefficient  $\alpha_E=\delta E/\delta H$ , and  $\alpha=\epsilon_o\epsilon_r\alpha_E$  where  $\epsilon_r$  is the relative permittivity.

Studies on ME composites were initiated in the early 1970s and were primarily on bulk samples of ferrimagnetic spinel ferrites and piezoelectric barium titanate.<sup>3</sup> Although ferrites are not piezomagnetic, magnetostriction in an ac magnetic field gives rise to pseudopiezomagnetic effects. The bulk composites yielded  $\alpha_E$  values that were two to three orders-of-magnitude smaller than theoretical predictions. Such low values are primarily due to low resistivity for ferrites, which (i) limits the electric field used for poling the composite and consequently a poor piezoelectric coupling and (ii) produces a leakage current that results in the loss of induced voltage. These difficulties could easily be eliminated in a layered composite.<sup>4-9</sup> The ease of poling allows enhancement of piezoelectric, and therefore, ME effects. Theoretical estimates of  $\alpha_E$  for a bilayer of ferrite-lead zirconate titanate are comparable to values for bulk composites.<sup>4,10</sup>

The largest  $\alpha_E$  ever achieved was reported recently in trilayers of terfenol and lead zirconate titanate (PZT).<sup>6</sup>

Ferrite-based layered systems studied so far include cobalt ferrite (CFO) or nickel ferrite (NFO) with PZT.<sup>4,7,9</sup> In particular, composites with CFO are of interest because of high magnetostriction. Such samples are prepared either by laminating and sintering thick films of ferrites and PZT or by gluing ferrite and PZT discs with silver epoxy.<sup>4</sup> Studies on CFO-PZT showed  $\alpha_E$  on the order of 75 mV/cm Oe, an order-of-magnitude larger than in bulk composites. But the measured values, however, are an order-of-magnitude smaller than theoretical values. Thus composites with magnetically hard CFO showed weak ME coupling in spite of high magnetostriction.<sup>3</sup> Nickel ferrite, on the other hand, is a soft ferrite with a much smaller anisotropy and magnetostriction than in CFO. In a very recent study on layered samples of NFO-PZT, we reported a giant ME coupling on the order of 1500 mV/cm Oe and  $\alpha_E$  values in excellent agreement with theory.<sup>7</sup> These observations are indicative of the influence of magnetic parameters such as anisotropy, initial permeability, and magnetostriction on ME effects. In particular, the magnetomechanical coupling that gives rise to ME effects is dependent on the domain dynamics and ac magnetostriction.

This work is directed toward an understanding of the effects of magnetic parameters of ferrites on ME coupling in multilayers with PZT. It is possible to accomplish controlled variations in the ferrite parameter with Zn substitution. The following oxides were used for the magnetic phase: cobalt zinc ferrite  $\text{Co}_{1-x}\text{Zn}_x\text{Fe}_2\text{O}_4$  (CZFO) ( $x=0-0.6$ ) and nickel zinc ferrite  $\text{Ni}_{1-x}\text{Zn}_x\text{Fe}_2\text{O}_4$  (NZFO) ( $x=0-0.5$ ). Commercially available PZT was used for the piezoelectric phase. Layered samples were prepared by lamination and sintering of ferrite and PZT thick films obtained by tape casting. X-ray-diffraction studies indicated the absence of any impu-

rities, but the PZT lattice was strained. The strain was large in CZFO-PZT compared to NZFO-PZT and it decreased with increasing Zn substitution. Magnetic and electrical parameters for the composites were in general agreement with bulk values. Magnetoelectric voltage coefficients were measured for transverse ( $\delta E$  perpendicular to  $\delta H$ ) and longitudinal ( $\delta E$  parallel to  $\delta H$ ) field orientations for frequencies 10–1000 Hz.

The present study provides clear evidence for strengthening of ME effects with the substitution of Zn, with the largest increase for CZFO-PZT and the smallest increase for NZFO-PZT. In most of the samples studied, we observe a transverse ME coupling that is an order-of-magnitude stronger than the longitudinal coupling due to relative strengths of the piezomagnetic effects. In CZFO-PZT,  $\alpha_E$  increases as the Zn concentration is increased and shows a maximum for  $x=0.4$ . The coupling weakens with further increase in Zn concentration. A similar but a smaller Zn-substitution-related increase of  $\alpha_E$  is evident in NZFO-PZT. These data were analyzed using our recent model for a bilayer of ferrite-PZT. The model facilitates the estimation of the strength of interface coupling  $k$  between the two phases, with  $k=1$  for an ideal interface and 0 for a frictionless case. For CZFO-PZT,  $k$  values are small and show an increase with Zn concentration. A perfect coupling is inferred for NZFO-PZT. These results are discussed in terms of dependence of  $k$  on structural, mechanical, chemical, and electromagnetic parameters for the two phases. We infer from the analysis that enhancement in ME coupling with Zn substitution is related to a reduction in magnetic anisotropy, leading to high permeability and, therefore, a strong magnetomechanical effect in the ferrite. The multilayer ferrite-PZT composites studied here are of interest for use as sensors and in high-frequency devices.

## II. SAMPLE PREPARATION AND STRUCTURAL, MAGNETIC, AND ELECTRICAL CHARACTERIZATION

Multilayer samples of NZFO-PZT and CZFO-PZT were synthesized using thick films of ferrites and PZT obtained by tape casting.<sup>11</sup> The ferrite powder necessary for tape casting was prepared by the standard ceramic techniques that involved mixing the oxides or carbonates of the constituent metals, followed by presintering and final sintering. A ball mill was used to grind the powder to submicron size. For PZT films, we used commercially available powder.<sup>12</sup> The fabrication of thick films contained the following main steps: (i) preparation of cast of constituent oxides, (ii) deposition of 10–40- $\mu\text{m}$ -thick-film tapes by doctor blade techniques, and (iii) lamination and sintering of composites. Ferrite or PZT powders were mixed with a solvent (ethyl alcohol), plasticizer (butyl benzyl phthalate), and binder (polyvinyl butyral) in a ball mill for 24 h. The slurries were cast into 10-40- $\mu\text{m}$  tapes on silicon-coated mylar sheets using a tape caster. The films were dried in air for 24 h, removed from the mylar substrate, and arranged to obtain the desired structure. They were then laminated under high pressure (3000 psi) and high temperature (400 K), and sintered at 1375–1475 K. Multilayers consisted of  $(n+1)$  layers of ferrites and  $n$  layers of PZT ( $n=5-30$ ). Samples of CZFO-PZT were sintered at

the low end of the sintering temperature range to minimize warping. The samples were characterized in terms of structural, electric, magnetic, and magnetoelectric parameters.

The surface morphology and cross section of the samples were examined with a high-resolution ( $\times 1000$ ) metallurgical microscope. Samples contained fine grains and some open pores. The porosity ranged from 5% to 10% depending on the processing temperature. In particular, CZFO-PZT samples showed high porosity. The cross-section studies showed well-bonded structure with uniform thickness for ferrite and PZT. Structural characterization was carried out on sintered multilayers and powdered samples using an x-ray diffractometer. Data for sintered composites did not show any epitaxial or textured nature for the films. Data for powdered samples showed two sets of well-defined peaks; the first set of narrow peaks corresponded to the magnetic phase (NZFO or CZFO), while the second set of relatively broad peaks was identified with the piezoelectric phase (PZT). Main peaks of both sets were of nearly equal intensity. The key inference from x-ray-diffraction studies is that no detectable new (impurity) phases are formed because of anticipated diffusion at the interface.

The structural parameters for bulk ferrites, and ferrite and PZT films in the layered samples, were calculated from the x-ray data and are shown in Fig. 1. The figure also shows the Zn concentration dependence of the full width at half maximum (FWHM) for the most intense ferrite and PZT diffraction peaks for the composites. Both bulk and thick films of ferrites have a cubic spinel structure and the lattice constants increase linearly with Zn concentration, in very good agreement with reported values.<sup>13</sup> The narrowness of the peaks and the estimated lattice parameters indicate that the spinel structure is preserved and that the ferrite layers are free of interface strain. But the situation is different for PZT. Bulk PZT is found to be tetragonal with  $a=0.4062(5)$  and  $c=0.4105(6)$  nm, and a FWHM of  $0.3^\circ$  for the (110) peak. The data in Fig. 1 show a general broadening of the PZT peaks in the composites. Although the  $c$  value for PZT is unchanged in the layered samples, the data shows a smaller  $a$  value for both series of multilayers. In NZFO-PZT, the reduction in  $a$  amounts to 1% in the unit-cell volume of PZT and it remains independent of Zn. A larger volume reduction, as much as 2.5%, occurs in CZFO-PZT. One also notices a linear increase in the  $a$  value with Zn concentration in CZFO-PZT. Thus x-ray data imply a strained PZT in the heterostructures. The strain is rather large in CZFO-PZT compared to NZFO-PZT.

Magnetic characterization included magnetization with a Faraday balance and a vibrating sample magnetometer, ferromagnetic resonance at the  $x$  band, and magnetostriction with a strain gage. The saturation magnetization  $M_s$  was found to agree with bulk values and increased initially with Zn substitution for  $x=0-0.4$ , followed by a decrease for higher Zn substitution.<sup>13</sup> For CZFO-PZT samples, there was a significant dependence of magnetization on magnetic-field orientation due to the expected high magnetic anisotropy. Investigation of ferromagnetic resonance (FMR) in composites was carried out using a spectrometer operating at 9.8 GHz. The derivative of the microwave absorption line as a

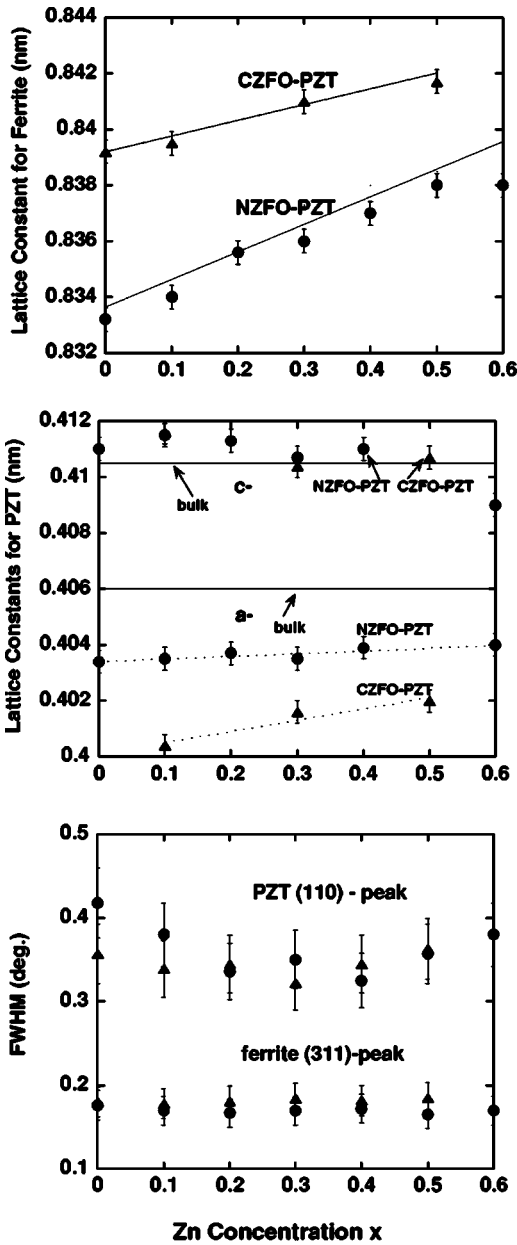


FIG. 1. Lattice constants and the full width at half maximum (FWHM) as a function of Zn substitution  $x$  for ferrites and lead zirconate titanate (PZT) in multilayer composites. The solid lines are lattice constants for bulk nickel zinc ferrite,  $\text{Ni}_{1-x}\text{Zn}_x\text{Fe}_2\text{O}_4$  (NZFO), cobalt zinc ferrite,  $\text{Co}_{1-x}\text{Zn}_x\text{Fe}_2\text{O}_4$  (CZFO), and PZT. The triangles and circles in the upper part are  $a$  values for the cubic spinels CZFO and NZFO, respectively, in the multilayers. The middle part shows the tetragonal  $a$  and  $c$  values for PZT in NZFO-PZT (circles) and CZFO-PZT (triangles). The lower part shows the FWHM values for the (110) diffraction peak for PZT and the (311) peak for CZFO (triangles) and NZFO (circles) in the composites.

function of the magnetic field was registered for the static field  $H$  parallel and perpendicular to the sample plane. Absorption spectra for CZFO-PZT had a very wide and irregular shape, while NZFO-PZT had rather narrow and symmetrical lines. This correlates with observed hysteresis and coercivity in magnetization for CZFO-PZT and their absence

for NZFO-PZT. Data on ferromagnetic resonance fields were used to estimate the anisotropy field  $H_A$ . For NZFO-PZT, it varied from 400 Oe for  $x=0$  to 50 Oe for  $x=0.5$ . For CZFO-PZT,  $H_A$  decreased from 3.7 kOe to 400 Oe as  $x$  was increased from 0 to 0.5. Magnetostriction was measured with the standard strain gage technique and detailed data are provided in Sec. IV. Measurements of electrical resistance  $R$  and capacitance  $C$  were carried out to probe the quality of the composites. The  $R$  and  $C$  were smaller than expected values due to either higher than expected conductivity of PZT films or the presence of “shorts” in the PZT films. The ferroelectric-to-paraelectric transition temperature of 600 K agreed with the bulk value.<sup>14</sup> Further details on magnetic and electrical characterization are provided in Refs. 14 and 15.

### III. MAGNETOELECTRIC EFFECTS

Samples were polished; electrical contacts were made with silver paint, and poled. The poling procedure involved heating the sample to 420 K and the application of an electric field  $E$  of 20 kV/cm. As the sample was cooled to 300 K,  $E$  was increased progressively to 50 kV/cm over 30 min. The piezoelectric coupling coefficient was measured with a  $d_{33}$  meter. The parameter of importance for the multilayers is the magnetoelectric voltage coefficient  $\alpha_E$ . Magnetoelectric measurements are usually performed under two distinctly different conditions: the induced magnetization is measured for an applied electric field or the induced polarization is obtained for an applied magnetic field. We measured the electric field produced by an alternating magnetic field applied to a biased composite. The samples were placed in a shielded three-terminal sample holder and placed between the pole pieces of an electromagnet that was used to apply a bias magnetic field  $H$ . The required ac field of  $\delta H = 1$  Oe at 10–1000 Hz parallel to  $H$  was generated with a pair of Helmholtz coils. The resulting ac electric field  $\delta E$  perpendicular to the sample plane was estimated from the voltage  $\delta V$  measured with a lock-in amplifier. The ME voltage coefficient  $\alpha_E = \delta V / t \delta H$  where  $t$  is the *effective thickness* of PZT. The measurements were done for two different field orientations. With the sample plane represented by (1, 2), the transverse coefficient  $\alpha_{E,31}$  was measured for the magnetic fields  $H$  and  $\delta H$  along direction 1 (parallel to the sample plane) and perpendicular to  $\delta E$  (direction 3). The longitudinal coefficient  $\alpha_{E,33}$  was measured for all the fields perpendicular to the sample plane. Magnetoelectric characterization was carried out as a function of frequency and bias magnetic field  $H$ .

Studies were performed on multilayers with equal thickness for ferrite and PZT (10–40  $\mu\text{m}$ ) and a series of  $n$  values. First we consider samples of CZFO-PZT. Figure 2 shows representative data on the  $H$  dependence of  $\alpha_{E,31}$  and  $\alpha_{E,33}$  for a sample in which 40% Co is replaced by Zn. The data at room temperature and 100 Hz are for a sample with  $n = 10$ . As the bias field is increased from zero,  $\alpha_E$  increases rapidly to a peak value. With further increase in  $H$ , the ME coefficients drop to a minimum or zero value. When  $H$  is reversed, we observed (i) a 180° phase difference relative to the ME voltage for  $+H$  and (ii) a small decrease in the peak

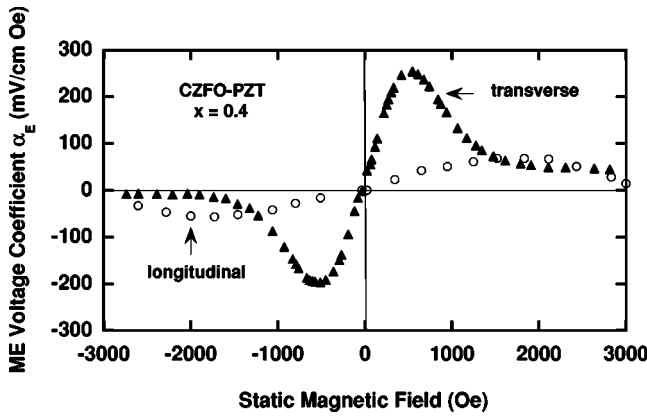


FIG. 2. Magnetoelectric (ME) voltage coefficient  $\alpha_E = \delta E / \delta H$  versus bias magnetic field  $H$  for a multilayer of CZFO ( $x=0.4$ ) PZT. The sample contained 11 layers of CZFO and 10 layers of PZT with a thickness of  $18 \mu\text{m}$ . The data at room temperature and 100 Hz are for transverse (out-of-plane  $\delta E$  perpendicular to in-plane  $\delta H$ ) and longitudinal (out-of-plane  $\delta E$  and  $\delta H$ ) field orientations. There is  $180^\circ$  phase difference between voltages for  $+H$  and  $-H$ .

value for  $\alpha_E$  compared to the value for  $+H$ . There was no noticeable hysteresis or remanence in  $\alpha_E$  vs  $H$ . As discussed later, the  $H$  dependence in Fig. 2 essentially tracks the strength of piezomagnetic coupling  $q = d\lambda/dH$  where  $\lambda$  is the magnetostriction for the ferrite. The coupling vanishes when  $\lambda$  attains saturation. Consider next the  $H$  dependence of transverse and longitudinal coefficients. Although overall features in Fig. 2 are similar for both cases, one finds the following differences. (i) The initial rate of increase in  $\alpha_E$  with  $H$  is much higher for the transverse case than for longitudinal orientation for the fields. (ii) The peak  $\alpha_{E,31}$  is a factor-of-5 higher than  $\alpha_{E,33}$ . (iii) The peak value in  $\alpha_{E,33}$  occurs for a higher bias field than for the transverse case. These observations could be understood in terms of  $H$  variation of parallel and perpendicular magnetostriction for the ferrite.

Similar  $\alpha_E$  vs  $H$  data were obtained for samples with  $x$  values varying from 0 to 0.6. Both  $\alpha_{E,31}$  and  $\alpha_{E,33}$  were measured. Figure 3 shows the room-temperature variation of

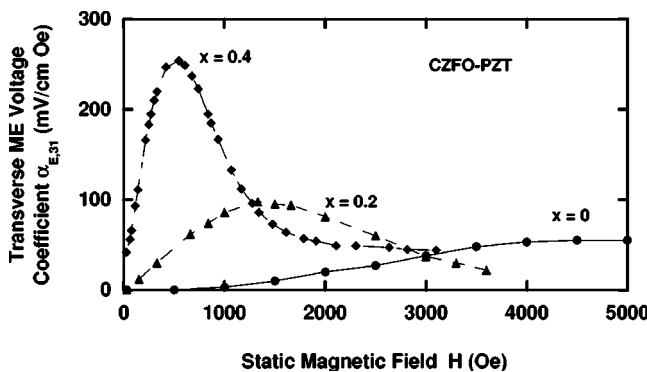


FIG. 3. Transverse ME voltage coefficient  $\alpha_{E,31}$  as a function of  $H$  at room temperature and 100 Hz for multilayers of CZFO-PZT with  $x=0, 0.2,$  and  $0.4$ .

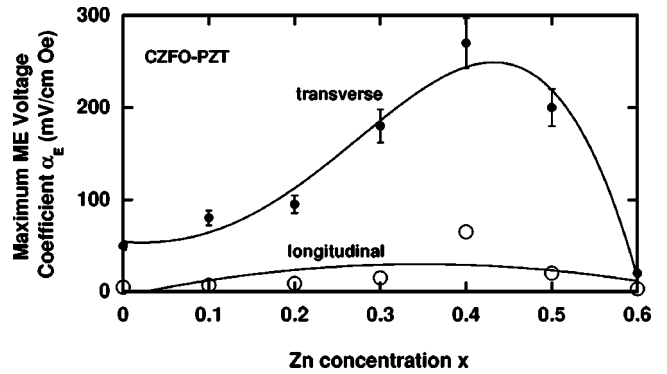


FIG. 4. Variation of peak transverse and longitudinal ME voltage coefficients with zinc concentration  $x$  in layered CZFO-PZT. The data at room temperature and 100 Hz were obtained from profiles as in Figs. 2 and 3. The bars indicate the range of measured values. The solid lines are to guide the eyes.

$\alpha_{E,31}$  with  $H$  for  $x=0-0.4$ . Data on the longitudinal coupling are not shown since the coupling was quite weak for all  $x$  values except for 0.4. As  $x$  is increased one notices (i) an increase in the rate at which  $\alpha_{E,31}$  varies with  $H$  at low fields, (ii) the peak in  $\alpha_{E,31}$  occurs at progressively decreasing  $H$ , and (iii) there is a general increase in the peak value of  $\alpha_{E,31}$ . In Fig. 4 the variation of maximum  $\alpha_E$  with  $x$  is shown for both transverse and longitudinal cases. The peak coefficients were measured for several samples and the figure shows the range of measured values and their average. As the Zn substitution is increased, one observes a sharp increase in  $\alpha_{E,31}$ , from 50 mV/cm Oe for  $x=0$  to 280 mV/cm Oe for  $x=0.4$ . Further increase in  $x$  is accompanied by a substantial reduction in  $\alpha_{E,31}$ . The longitudinal coupling parameter is very weak for the entire series. One needs to compare the results in Figs. 2–4 with past studies on bulk samples of CFO-BaTiO<sub>3</sub> and CFO-PZT and multilayers of CFO-PZT.<sup>16</sup> Bulk samples showed very weak ME interactions but layered CFO-PZT showed  $\alpha_E$  of 75 mV/cm Oe, comparable to values in Fig. 3.<sup>16</sup> It is obvious from the present study that Zn substitution in cobalt ferrite is a key ingredient for strong ME coupling in multilayers. We attribute the efficient field conversion properties to modification of magnetic parameters due to Zn (Sec. IV).

Similar ME studies were performed on nickel zinc ferrite-PZT samples with  $x=0-0.5$ . Figure 5 shows representative data on the  $H$  dependence of  $\alpha_E$  for NZFO-PZT samples with  $x=0-0.4$ . The data were obtained on samples with  $n=10-15$ . For NFO-PZT ( $x=0$ ),  $\alpha_{E,31}$  vs  $H$  shows the expected resonancelike character with a maximum centered at  $H=400$  Oe. When Zn is substituted for Ni, we notice an increase in the peak value of  $\alpha_{E,31}$  for low  $x$  values. As  $x$  is increased, a downshift is observed in the  $H$  value corresponding to maximum  $\alpha_{E,31}$ . The magnetic-field range for strong ME effects decreases with increasing Zn content. Data on the longitudinal coupling in Fig. 5 shows the following important departures from the transverse case. (i) The coupling strength does not show any dependence on  $x$  for low Zn substitution. (ii) As  $x$  is increased, an upshift is observed for the  $H$  value corresponding to peak  $\alpha_{E,33}$ . (iii) The ME

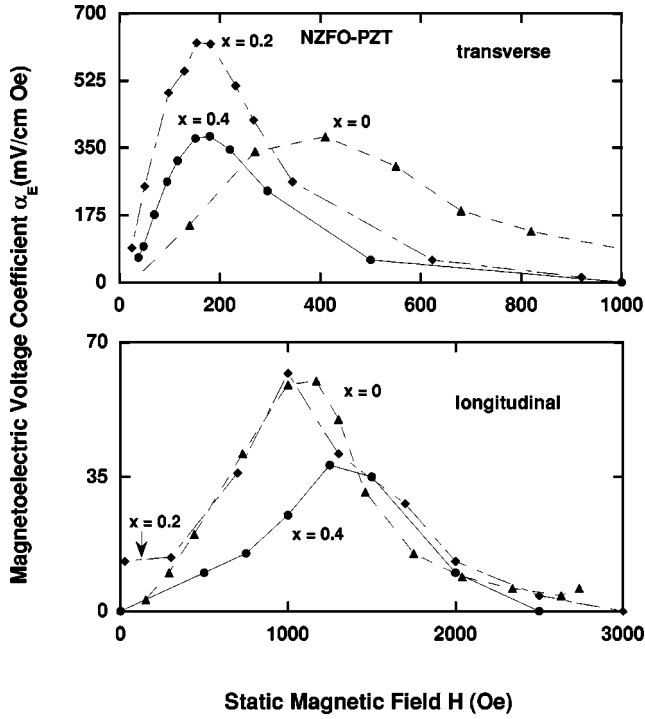


FIG. 5. ME voltage coefficients versus  $H$  data as in Fig. 2, but for multilayer samples of NZFO-PZT.

coupling is realized over a wide field interval. Similar  $\alpha_E$  vs  $H$  profiles were obtained for other  $x$  values. The variations of maximum  $\alpha_E$  with  $x$  are plotted in Fig. 6. The range of measured  $\alpha_E$  and the average values are shown. The data reveal a 60% increase in the transverse ME voltage coefficient as  $x$  is increased from 0 to 0.2, followed by a reduction in  $\alpha_{E,31}$  for higher  $x$ . The longitudinal coefficient also shows a similar behavior. The  $\alpha_E$  values are significantly higher than reported values in past studies on bulk or layered samples. The coupling coefficient must be compared with 80 for NFO-barium titanate,<sup>3</sup> 115 for NFO-PZT bulk composites,<sup>6</sup> and 300–400 mV/cm Oe for NFO-PZT multilayers.<sup>5,7,9</sup>

Now we compare and contrast the ME voltage coefficient data for the two series of samples. The strongest ME couplings are observed for NZFO-PZT. The highest ME voltage coefficients are measured for Zn substitutions in the range  $x=0.2$ – $0.4$ , depending on the nature of ferrite. Although

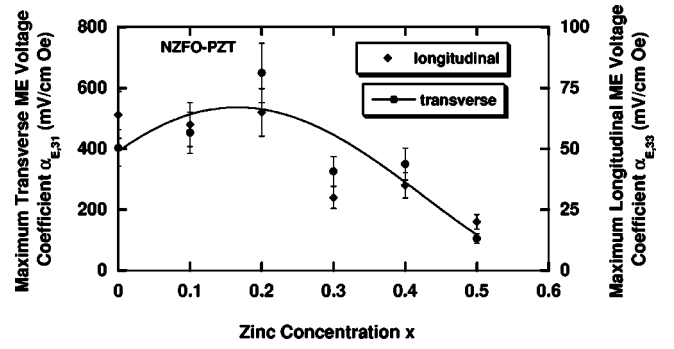


FIG. 6. Zinc concentration dependence of maximum transverse and longitudinal ME coefficients in NZFO-PZT layered samples. The line is to guide the eye.

both systems show enhancement in the strength of ME coupling with Zn substitution, the largest increase occurs for CZFO-PZT samples. The ME coupling is present over a wide  $H$  interval in CZFO-PZT. One observes a dramatic shift in the  $H$  value corresponding to peak  $\alpha_{E,31}$  for CZFO-PZT.

#### IV. DISCUSSION

We first estimate the magnetoelectric voltage coefficients and their magnetic-field dependence for comparison with data. Following this, possible causes of zinc-substitution-related effects on ME coupling are considered. Harshe *et al.* proposed a model for ME effects in a two-layer structure.<sup>4</sup> Ideal coupling was assumed at the interface and an expression was obtained for the longitudinal ME voltage coefficient. The major deficiencies of the model are as follows. (i) For the longitudinal case, important effects related to finite magnetic permeability for the ferrite were ignored. A reduction in the internal magnetic field and weakening of ME interactions are expected due to demagnetizing fields. (ii) The model did not consider ME coupling under transverse field orientations for which studies show a giant ME effect. (iii) It is necessary to consider less-than-ideal interface coupling. We recently developed a comprehensive theory in which the composite is considered as a homogeneous medium with piezoelectric and magnetostrictive subsystems.<sup>10</sup> A novel technique was employed to take into account the actual interface conditions, i.e., by introducing an interface coupling parameter  $k$ . Using open circuit conditions, one obtains the following expressions for the longitudinal and transverse ME voltage coefficients:

$$\alpha_{E,33} = \frac{-2\mu_0 k(1-\nu)^p d_{31}^m q_{31}}{2(p d_{31})^2(1-\nu)k + p \epsilon_{33}^T [(p s_{11} + p s_{12})(\nu-1) - k\nu(m s_{11} + m s_{12})]} \times \frac{[(p s_{11} + p s_{12})(\nu-1) - k\nu(m s_{11} + m s_{12})]}{[\mu_0(\nu-1) - m \mu_{33}\nu][k\nu(m s_{11} + m s_{12}) - (p s_{11} + p s_{12})(\nu-1)] + 2(m q_{31})^2 k \nu^2}, \quad (1)$$

$$\omega_{E,31} = \frac{-k(\nu-1)^p d_{31}^m (q_{11} + m q_{21})}{(m s_{11} + m s_{12})^p \epsilon_{33}^T k \nu + (p s_{11} + p s_{12})^p \epsilon_{33}^T (1-\nu) - 2(p d_{31})^2 k(1-\nu)}. \quad (2)$$

Here  $m$  denotes the magnetostrictive phase and  $p$  the piezoelectric phase,  $d$  and  $q$  are the piezoelectric and piezomagnetic coupling coefficients, respectively,  $s$  is the compliance coefficient,  $\epsilon^T$  is permittivity at constant stress,  $\mu$  is the tensor permeability, and  $v = v^p / (v^p + v^m)$  with  $v^p$  and  $v^m$  denoting the volume of piezoelectric and magnetostrictive phases, respectively. The interface coupling parameter  $k$  that describes the actual boundary condition is defined by  $k = (pS_i - pS_{i0}) / (mS_i - pS_{i0})$  where  $S$  are the strain tensor components and  $S_{i0}$  is the strain with no friction. The  $k$  value depends on interface quality, with  $k=1$  for ideal coupling between the layers and 0 for the case with no friction.

Apart from other materials parameters, we require the knowledge of the piezomagnetic coupling constants  $q = \delta\lambda / \delta H$ , where  $\lambda$  is the magnetostriction. One needs the magnitude of  $q$  and its variation with  $H$  for the estimation of field dependence of  $\alpha_E$ . The magnetostriction  $\lambda_{13}$  (in-plane magnetostriction for  $H$  perpendicular to the sample plane) and its derivative with  $H$ ,  $q_{13}$  were quite small for both CZFO-PZT and NZFO-PZT, resulting in weak  $\alpha_{E,33}$ . The demagnetization when  $H$  and  $\delta H$  are perpendicular to the sample plane further reduces the ME voltage coefficient.<sup>10</sup> Consequently, the longitudinal ME coupling is expected to be much weaker than in the transverse case, as is the case for data in Figs. 2–6. The discussion to follow is therefore restricted to the transverse ME effect.

We determined  $q$  values from data on  $\lambda$  vs  $H$  for pure and Zn-substituted ferrites. Representative data on  $\lambda_{11}$  (in-plane parallel magnetostriction) and  $\lambda_{12}$  (in-plane perpendicular magnetostriction) are shown in Figs. 7 and 8 for CZFO and NZFO, respectively. The measurements were made at room temperature on ferrites ( $1 \times 1 \times 0.05$  cm) made from thick films. A (Measurement Group) strain gage and a strain indicator were used. Consider the magnetostriction in Fig. 7 for CZFO samples. For  $x=0$ , as  $H$  is increased, we find a weak increase in the magnitude of  $\lambda$  for fields up to 2 kOe and it is followed by a strong increase for higher  $H$ . The saturation of  $\lambda_{11}$  occurs at 5 kOe, but the perpendicular magnetostriction does not show any saturation. When 20% Co is replaced with Zn, one observes a rather dramatic strengthening of low-field piezomagnetic coupling in the ferrite. The magnetostriction increases rapidly with  $H$  for fields up to 1.5 kOe. The saturation occurs at a much lower  $H$  compared to CFO. Further increase in  $x$  results in a decrease in  $\lambda$ , but the low-field  $q$  remains high since the saturation  $H$  decreases progressively with increasing  $x$ . For  $x=0.4$ , one measures a saturation value of  $\lambda_{12}$  that is higher than  $\lambda_{11}$ . Thus the introduction of Zn in CFO leads to overall strengthening of low-field piezomagnetic coupling. Data on magnetostriction for NZFO-PZT are shown in Fig. 8. The changes in  $\lambda$  with Zn substitution are less dramatic than in CFO. For  $x=0$ ,  $\lambda_{11}$  is negative and large, but the perpendicular magnetostriction is positive and very small. With increasing  $x$ , data show an overall decrease in the saturation  $\lambda$  and  $H$  value for saturation. For  $x=0.2$ , the low-field piezomagnetic coupling is stronger than in NFO.

We now use the bilayer model for theoretical estimates of  $\alpha_{E,31}$  for comparison with the data. The following bulk values were used in Eq. (2) for the composite parameters:

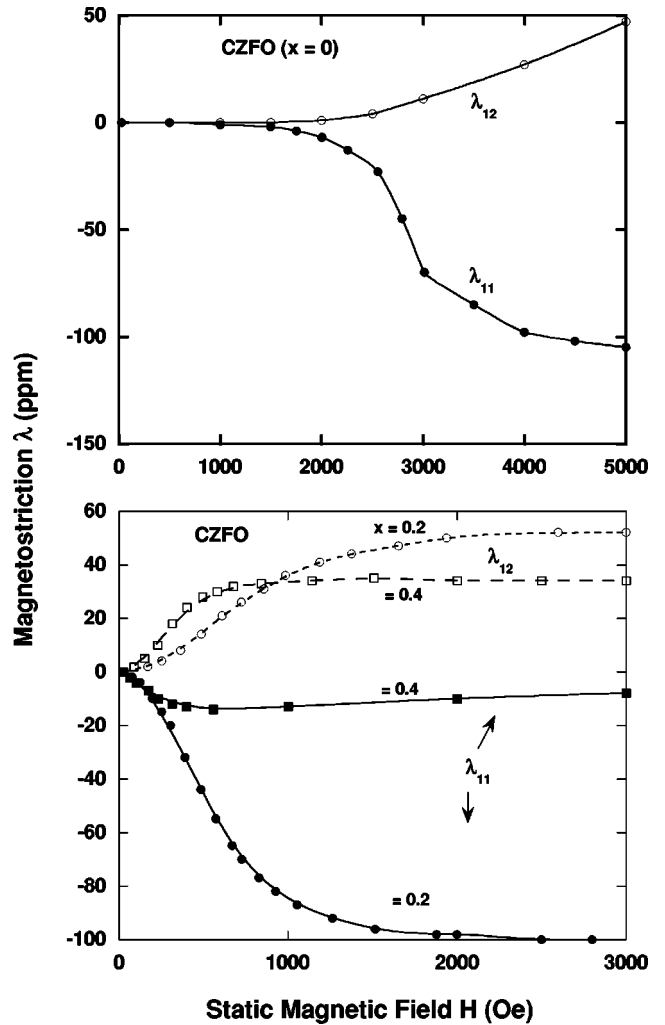


FIG. 7. Room-temperature in-plane parallel ( $\lambda_{11}$ ) and perpendicular ( $\lambda_{12}$ ) magnetostriction versus  $H$  for CZFO bulk samples ( $x=0, 0.2, 0.4$ ) made from thick films.

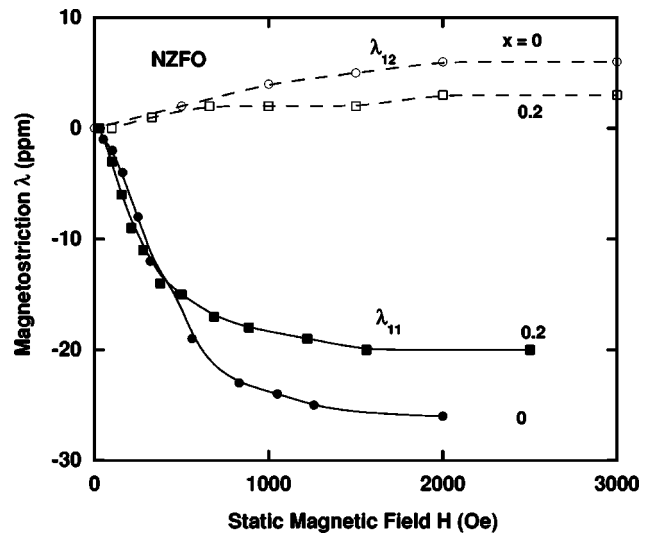


FIG. 8. Magnetostriction vs  $H$  data (as in Fig. 7) for NZFO for  $x=0$  and 0.2.

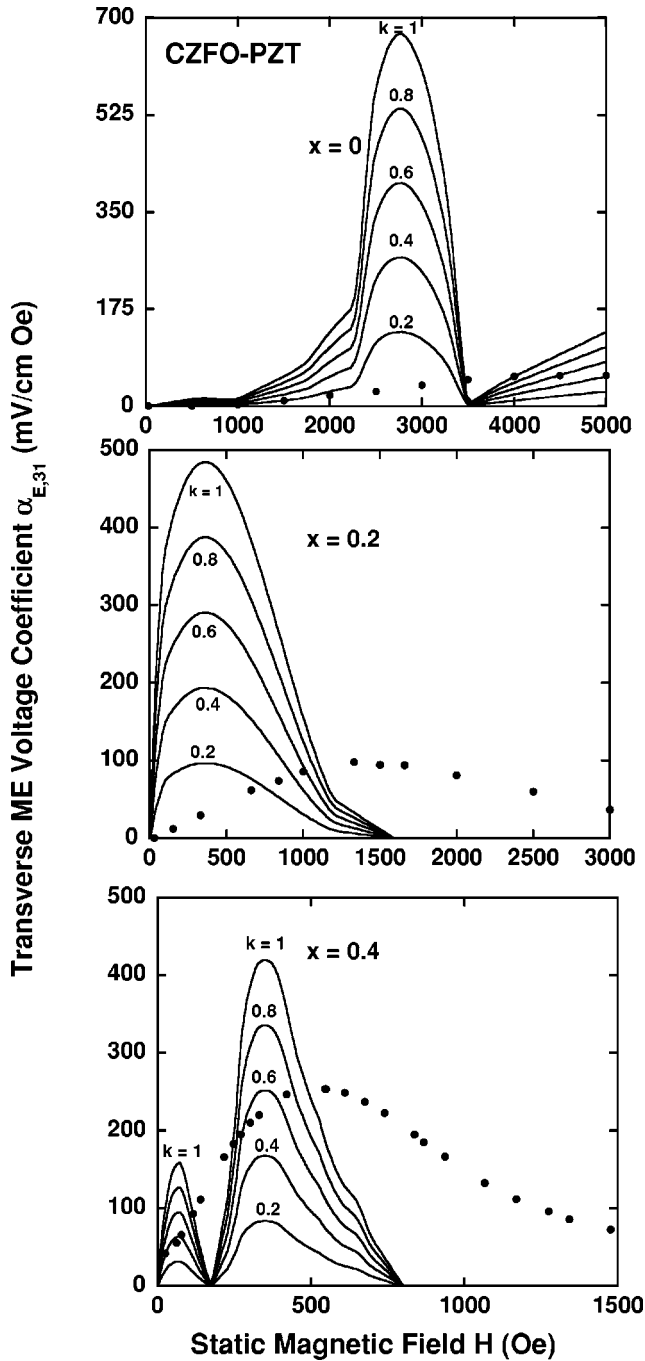


FIG. 9. Comparison of theoretical and measured values of the transverse ME voltage coefficient  $\alpha_{E,31}$  for layered samples of CZFO ( $x=0, 0.2, 0.4$ )-PZT. The solid curves are theoretical values for a series for interface coupling parameter  $k$ .

$p_{S11} = 15 \times 10^{-12}$ ,  $p_{S12} = -5 \times 10^{-12}$ ,  $m_{S11} = 6.5 \times 10^{-12}$ , and  $m_{S12} = -2.4 \times 10^{-12}$  m<sup>2</sup>/N, and  $\epsilon_{33}/\epsilon_0 = 1750$ .<sup>4,12,13</sup> The measured value for  $d_{33}$  in the bulk and layered samples was 250 pm/V, corresponding to  $d_{31} = d_{33}/2 = 125$  pm/V. Data in Figs. 7 and 8 were fitted to a polynomial for the estimation of  $q$  and its  $H$  dependence. We assume  $\nu = 0.5$ , corresponding to equal volume of ferrites and PZT. Calculated values of  $\alpha_{E,31}$  are compared in Fig. 9 with the data for CZFO-PZT samples. Results on  $\alpha_{E,31}$  vs  $H$  are shown as a function of the interface

coupling constant  $k$  for samples with  $x=0, 0.2$ , and  $0.4$ . For CFO-PZT ( $x=0$ ), the theory predicts a gradual increase in  $\alpha_{E,31}$  with increasing  $H$ . A maximum in  $\alpha_{E,31}$  is expected for a field of 2.8 kOe and the ME coefficient drops down to zero for  $H=3.5$  kOe, the field at which  $(q_{11}+q_{12})$  vanishes. Above this field the effective  $q$  is once again nonzero and it gives rise to a ME voltage. Upon increasing  $x$  from 0 to 0.2, significant theoretical predictions concern a rapid increase in the low field  $\alpha_{E,31}$ , a downshift in the peak position to 400 Oe, and a maximum  $\alpha_{E,31}$  that is 30% smaller than for  $x=0$ . Finally, for  $x=0.4$ , the calculated  $\alpha_{E,31}$  vs  $H$  reveals an intermediate minimum, as for  $x=0$ . The maximum  $\alpha_{E,31}$  is the smallest of the three compositions considered in Fig. 9.

Next we compare the data and theoretical values of  $\alpha_{E,31}$  for CZFO-PZT. For  $x=0$ , we observe a substantial disagreement between theory and data. Neither the magnitude of  $\alpha_{E,31}$  for  $k=1$  nor its  $H$  dependence agree with the data. The predicted values for perfect interface coupling are an order-of-magnitude higher and  $H$  values for maximum  $\alpha_{E,31}$  are a lot smaller than measured values. A weak interface coupling, with  $k$  on the order of 0.1, is evident for  $x=0$ . We notice a similar behavior for  $x=0.2$ . Magnitudes of theoretical  $\alpha_{E,31}$  for  $k=0.2$  are in agreement with the data, indicative of a stronger interface coupling than that in  $x=0$ . A significant inference from Fig. 9 is further strengthening of coupling for  $x=0.4$ . Even though the data does not show the predicted intermediate minimum in  $\alpha_{E,31}$ , the estimated magnitude and  $H$  dependence for  $k=0.6$  are in reasonable agreement with the data. A general improvement in the ME coupling is thus accomplished with Zn substitution in the ferrite.

A similar calculation and comparison for NZFO-PZT samples, however, indicate very good agreement between theory and data for pure nickel ferrite and the entire series of Zn substitution. Representative results are shown in Fig. 10 for  $x=0$  and 0.2. Theoretical estimates are for  $q$  values obtained from magnetostriction data in Fig. 8 and other material parameters mentioned earlier for ferrites. The data were obtained on multilayers with  $n=15$  and a layer thickness of 15  $\mu\text{m}$ . For NFO-PZT, one observes good agreement between theory for  $k=1$  and data. There is excellent agreement in the magnitude of  $\alpha_{E,31}$ , but the theory predicts a sharper drop in  $\alpha_{E,31}$  at high fields than that observed experimentally. For NZFO ( $x=0.2$ )-PZT, the figure shows theoretical  $\alpha_{E,31}$  smaller than measured values, but a very good agreement is evident for the  $H$  dependence of  $\alpha_{E,31}$ .

Consider now important features in Figs. 9 and 10 for the two systems. First, for CZFO-PZT, there is total lack of agreement between theory for  $k=1$  and data. Although magnetostriction data imply a strong piezomagnetic coupling, the estimated  $\alpha_{E,31}$  are factors-of-2–10 higher than measured values. Second, the introduction of Zn leads to an enhancement in the strength of interface coupling  $k$  and  $\alpha_E$ , in particular for CZFO-PZT. The constant  $k$  increases from 0.1 to 0.6 when Zn progressively replaces 40% of Co. The theory implies near perfect coupling for NZFO-PZT. Third, the theoretical value of  $H$  corresponding to the peak in  $\alpha_{E,31}$  is smaller than the measured values for all the compositions,

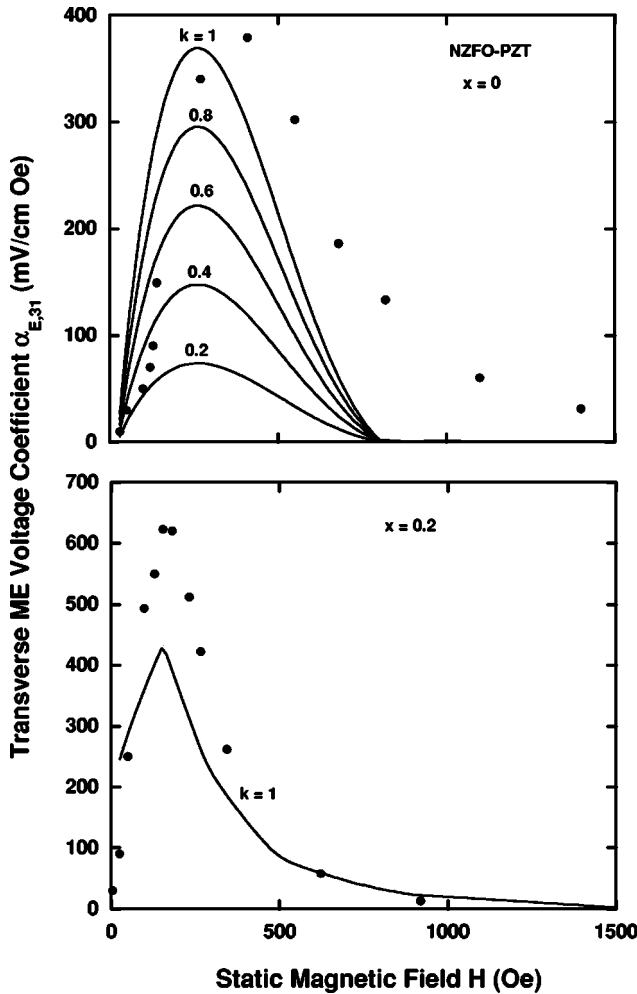


FIG. 10. Theoretical and measured  $\alpha_{E,31}$  versus  $H$  for NZFO ( $x=0, 0.2$ )-PZT composites.

except for NZFO ( $x=0.2$ )-PZT. Fourth, estimated high field  $\alpha_{E,31}$  are smaller than the data. The ME coefficient arises due to stress-mediated electromagnetic interactions at the interface and  $k$  is an important parameter for the composite. The theory and analysis presented here provide an elegant means to quantify an otherwise complex parameter  $k$ . We need to point out an important limitation of the model used here. The model is valid for a simple bilayer structure. It is necessary to extend the theory to include a multilayer consisting of  $n$  interfaces in a structure with  $(n+1)$ -ferrites and  $n$ -PZT layers. One expects a stronger interface coupling in multilayers than in bilayers.

Next we comment on the possible causes of inferred poor coupling in CZFO-PZT compared to NZFO-PZT, the system in which the coupling appears to be ideal. One expects  $k$  to be dependent on a variety of factors including structural, mechanical, chemical, and electromagnetic parameters. X-ray-diffraction data in Fig. 1 indicate the absence of any structural abnormalities. The ferrites and PZT retain their spinel and tetragonal structures, respectively. But the PZT diffraction peaks in the multilayers were broadened and shifted due to a lattice strain, primarily in the  $c$  plane. The distortion leads to a volume reduction that is small and inde-

pendent of Zn concentration in NZFO-PZT. The volume change in CZFO-PZT, however, is as high as 2.5% and is certain to influence the mechanical and electrical parameters for PZT and consequently  $k$  for the composite. With the substitution of Zn in CFO, data in Fig. 1 show a decreasing strain in PZT, accompanied by an improvement in the  $k$  value. Recall that theoretical  $\alpha_{E,31}$  values are for bulk values of the material parameters. These observations reinforce the need for the determination of material parameters, including the elastic constants, for the constituent phases in the layered composites.

Mechanical bonding at the interface that arises due to the high-temperature processing of the composite is another key factor that determines  $k$ . In some recent works, the bonding between magnetostrictive and piezoelectric media was accomplished with the use of silver epoxy.<sup>6</sup> The understanding of interface coupling in such cases is further complicated by the introduction of a foreign material. In our sintered composites it is difficult to quantify the strength of mechanical bonding. Simple peel tests are useful for such information, for example, in metal-polymer samples. We are not aware of such tests for sintered composites. One also expects  $k$  to be influenced by the possible presence of chemical inhomogeneities at the interface. An observation of importance in this regard is the deterioration in ME coupling in CZFO-PZT samples sintered at the high end of the temperature range 1375–1475 K. Although x-ray-diffraction data did not indicate any detectable levels of impurities, a “fused” interface and sample warping indicate microscopic chemical inhomogeneities in CZFO-PZT that will have an adverse impact on  $k$ .

Finally we address the anticipated effects of electromagnetic parameters on  $k$ . Even though the observed structural deformation of PZT will certainly impact  $k$ , one needs to focus on the effects of magnetostriction and magnetoelastic coupling for the following reasons. PZT is the only piezoelectric phase used in all the composites and its lattice is strained in both systems. The selection of composites and measurements are directed toward examining the role of ferrites on (i) ME voltage and (ii) the dependence of  $\alpha_{E,31}$  on  $H$ . There are two types of magnetostriction in a ferromagnet: (i) Joule magnetostriction associated with domain movements and (ii) volume magnetostriction associated with magnetic phase change. The volume magnetostriction is not important in the present situation since it is significant only at temperatures close to the Curie temperature. In ferrites domains are spontaneously deformed in the magnetization direction. Under the influence of a bias field  $H$  and ac field  $\delta H$ , domain-wall motion and domain rotation contribute to the Joule magnetostriction. Since the ME coupling involves dynamic magnetomechanical coupling, key requirements for the ferrite are unimpeded domain-wall motion, domain rotation, and a large  $\lambda$ . A soft, high, initial permeability (and low anisotropy as indicated by FMR studies) ferrite, such as NFO, is the key ingredient for strong ME effects. In magnetically hard cobalt ferrite, however, one has the disadvantage of a large anisotropy field that limits domain rotation. Our magnetization measurements yielded an initial permeability of 20 for NFO vs 3.5 for CFO. Figure 11 shows the

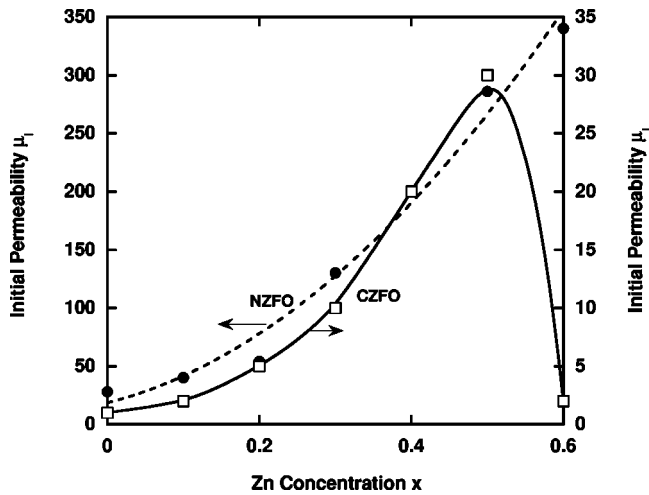


FIG. 11. Composition dependence of the initial permeability  $\mu_i$  (from Ref. 13) for CZFO and NZFO. The lines are to guide the eye.

composition dependence of the initial permeability  $\mu_i$  from Ref. 13 for CZFO and NZFO. With increasing Zn concentration in CZFO-PZT,  $\mu_i$  increases by a factor of 30 to a maximum value for  $x=0.5$  in agreement with anticipated reduction in the anisotropy. Recall that estimated  $H_A$  varied from 3.7 kOe to 400 Oe when Zn is varied from 0 to 0.4 in CZFO. For NZFO,  $\mu_i$  shows an order-of-magnitude increase for the composition range of importance. Even though  $\mu_i$  and  $\alpha_{E,31}$  track each other in CZFO-PZT, a similar behavior is absent in NZFO-PZT. It is clear that the important factor is not just  $\mu_i$ , but the magnetomechanical coupling  $k_m$  given by  $k_m = (4\pi\lambda'\mu_r/E)^{1/2}$  where  $\lambda'$  is the dynamic magnetostrictive constant and  $\mu_r$  is the reversible permeability, parameters analogous to  $q=(q_{11}+q_{12})$  and  $\mu_i$ , respectively, and  $E$  is the Young's modulus.<sup>17</sup> In Fig. 12, we compare maximum values of  $\alpha_{E,31}$  and the product  $\mu_i q$  as a function of  $x$  for both systems. The factors rise and fall in tandem and the maxima occur around the same composition, i.e.,  $x=0.2-0.3$  for NZFO-PZT and  $0.3-0.4$  for CZFO-PZT. Thus it is logical to associate the strong interface coupling for the entire series of NZFO-PZT and Zn-rich CZFO-PZT with efficient magnetomechanical coupling.

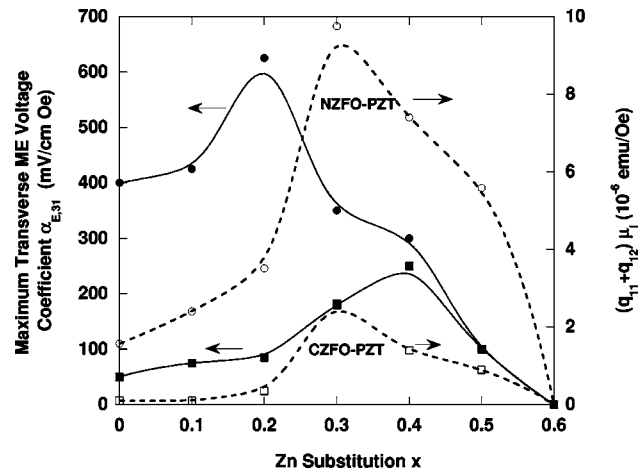


FIG. 12. Comparison of Zn-substitution dependence of maximum values of  $\alpha_{E,31}$  and the product  $q\mu_i$  for NZFO-PZT and CZFO-PZT. The parameter  $q=q_{11}+q_{12}$  is the net piezomagnetic coupling constant estimated from the slope of  $\lambda$  vs  $H$  data in Figs. 7 and 8.

## V. CONCLUSIONS

Studies on layered samples of zinc-substituted ferrites and PZT show evidence for efficient field conversion characteristics. The magnetoelectric voltage coefficient  $\alpha_E$  show an overall increase with increasing Zn concentration  $x$  in CZFO-PZT and NZFO-PZT. A maximum in  $\alpha_E$  occurs for  $x=0.2-0.4$ , depending on the ferrite. Analysis of the data using our model for a bilayer reveals ideal interface conditions for NZFO-PZT. The data imply poor coupling in CFO-PZT and a substantial improvement in samples with cobalt zinc ferrites. The Zn-assisted enhancement in ME coefficient is primarily due to low anisotropy and high permeability for the ferrites that results in favorable magnetomechanical coupling in the composites.

## ACKNOWLEDGMENT

The research was supported by a grant from the National Science Foundation (Grant No. DMR-0072144).

<sup>1</sup>D. N. Astrov, Zh. Eksp. Teor. Fiz. **38**, 984 (1960) [Sov. Phys. JETP **13**, 729 (1961)].

<sup>2</sup>J. Van Suchtelen, Philips Res. Rep. **27**, 28 (1972).

<sup>3</sup>J. Van den Boomgaard, D. R. Terrell, and R. A. J. Born, J. Mater. Sci. **9**, 1705 (1974); J. Van den Boomgaard, A. M. J. G. van Run, and J. van Suchtelen, Ferroelectrics **14**, 727 (1976); J. Van den Boomgaard and R. A. J. Born, J. Mater. Sci. **13**, 1538 (1978).

<sup>4</sup>G. Harshe, J. P. Dougherty, and R. E. Newnham, Int. J. Appl. Electromagn. Mater. **4**, 145 (1993); M. Avellaneda and G. Harshe, J. Intell. Mater. Syst. Struct. **5**, 501 (1994).

<sup>5</sup>T. G. Lupeiko, I. V. Lisnevskaya, M. D. Chkheidze, and B. I. Zvyagintsev, Inorg. Mater. (Transl. of Neorg. Mater.) **31**, 1245

(1995).

<sup>6</sup>J. Ryu, A. V. Carazo, K. Uchino, and H. Kim, J. Electroceram. **7**, 17 (2001); Jpn. J. Appl. Phys., Part 1 **40**, 4948 (2001).

<sup>7</sup>G. Srinivasan, E. T. Rasmussen, J. Gallegos, R. Srinivasan, Yu. I. Bokhan, and V. M. Laletin, Phys. Rev. B **64**, 214408 (2001).

<sup>8</sup>G. Srinivasan, E. T. Rasmussen, B. J. Levin, and R. Hayes, Phys. Rev. B **65**, 134402 (2002).

<sup>9</sup>S. Lopatin, I. Lopatina, and I. Lisnevskaya, Ferroelectrics **162**, 63 (1994).

<sup>10</sup>M. I. Bichurin, V. M. Petrov, and G. Srinivasan, J. Appl. Phys. **92**, 7681 (2002).

<sup>11</sup>R. E. Mistler and E. R. Twiname, Tape Casting: Theory and Practice (American Ceramic Society, Columbus, OH, 2000).

- <sup>12</sup>The PZT used in the study is sample number APC850, American Piezo Ceramics, Inc., Mackeyville, Pennsylvania.
- <sup>13</sup>*Numerical Data and Functional Relationships in Science and Technology, Group III, Crystal and Solid State Physics*, Vol. 4(b), *Magnetic and Other Properties of Oxides*, edited by K.-H. Hellwege and A. M. Springer, Landolt-Börnstein, New Series, Group III (Springer-Verlag, New York, 1970).
- <sup>14</sup>G. Srinivasan, A. A. Bush, K. E. Kamentsev, V. F. Meshcheryakov, and Y. K. Fetisov, *Appl. Phys. A* (to be published).
- <sup>15</sup>G. Srinivasan, R. Hayes, D. J. Fekel, V. M. Laletsin, and N. Paddubnaya, *Solid State Commun.* (to be published).
- <sup>16</sup>G. Harshe, Ph.D. thesis, The Pennsylvania State University, College Park, PA, 1991.
- <sup>17</sup>C. M. Van der Burgt, *Philips Res. Rep.* **8**, 91 (1953).